



Efficient Raman converter in the yellow range with high spatial and spectral brightness

MINH CHÂU PHAN HUY, PHILIPPE DELAYE, GILLES PAULIAT, AND SYLVIE LEBRUN**Laboratoire Charles Fabry, Institut d'Optique, CNRS, Univ Paris-Sud, 2 av. A. Fresnel, 91127 Palaiseau cedex, France***Corresponding author: sylvie.lebrun@institutoptique.fr**Received 7 June 2018; revised 16 July 2018; accepted 17 July 2018; posted 18 July 2018 (Doc. ID 332214); published 13 August 2018*

We present a Raman converter emitting at 583 nm on the second Stokes order of a line of propan-2-ol pumped by a microlaser at 532 nm in the sub-nanosecond regime. We used a mixture of liquids to adapt the transmission band of a photonic bandgap fiber. The internal conversion efficiency is 67% in photon numbers, and the output power is 1.06 mW, corresponding to a maximum peak power of 338 W. The beam delivered by the converter presents a Gaussian spatial structure and a high spectral brightness, typically more than five times higher than supercontinuum sources in this spectral range. © 2018 Optical Society of America

<https://doi.org/10.1364/AO.57.006892>

1. INTRODUCTION

Today there is a growing demand for pulsed, visible, and UV laser sources in biological applications using fluorescence, such as bioimaging and DNA sequencing, or environmental applications, such as atmospheric monitoring. In these areas compact laser systems which emit one or several “exotic” wavelengths with a good beam quality and a high spectral purity in the microjoule range would offer new opportunities. These might include exciting the increasing number of existing fluorophores [1,2], or realizing new microlasers [3]. Solutions such as supercontinuum sources [4–6] or optical parametric oscillators [7] are expensive, cumbersome, and oversized when only a few fixed discrete wavelengths are useful. Laser diodes can emit over a large number of wavelengths in the visible range but have many drawbacks, such as poor beam quality and low peak power in the pulsed regime, limited to a few tens of watts. Moreover, to sample the visible spectrum one needs to provide several laser diodes at the expense of extra costs. Microlasers are diode-pumped solid-state lasers emitting pulses in the microjoule range with a repetition rate that can vary from Hz to a few hundred of kHz. These lasers are very popular for their compactness and their user-friendly aspect, but commercial ones are mostly working at 1064 nm. They can be followed by a nonlinear stage to emit at 532 nm and possibly at 355 nm. Extending these achievable wavelengths to “on demand” discrete visible wavelengths would be of great interest for non-laser-specialized researchers. The Raman effect has been widely used to generate new wavelengths. Starting from a pump source at a fixed wavelength, reaching higher wavelengths is quite easy since the phase-matching condition is automatically satisfied. The Raman medium can be a crystal, a gas, or a liquid. With a crystal, the systems are quite complex and

not versatile. For example, in Ref. [8] in order to generate a given wavelength in the yellow range the authors need to develop a special pump source in the infrared based on the Raman effect at first and then insert a nonlinear crystal in the cavity for frequency doubling. Changing the emitted wavelength requires changing several components and realigning the whole system. The conversion efficiency remains quite low, typically a few percents. In order to increase the density of pump power over large interaction lengths, capillaries or special fibers filled with nonlinear liquids have been studied [9,10]. Even if the total conversion efficiency of the pump towards the Stokes lines can be high the energy of the pump is spread over all these lines generated through the Raman cascade effect. In order to stop this cascade effect and to optimize the transfer of energy of the pump to a given Stokes order, we propose to use hollow-core photonic crystal fibers (HC-PCF) filled with liquids. In such fibers, light can propagate in the core over long distances on small areas with low losses even if the refractive index of the core is smaller than the one of silica [11]. Multiline UV and visible Raman converters in hydrogen-filled HC-PCF have been fabricated [12]. In this reference, many Raman lines and Stokes orders are excited at the same time giving birth to 8–23 new wavelengths according to the fiber that is used. The use of liquids with a refractive index different from unity offers another degree of freedom. In HC-PCF the photonic bandgap guidance opens spectral transmission bands that can be adapted through the control of the refractive index of the material that fills the holes [13]. In previous works, we demonstrated the efficient conversion of the pump to a single Stokes order in a HC-PCF filled with ethanol by stopping the Raman cascade at the first Stokes order [14–16]. The pump source emitted at 532 nm sub-nanosecond μ J pulses, and the conversion efficiency at high pump power to the first Stokes

order of ethanol at 630 nm was 70% in photon numbers [15]. In particular we showed that although the liquid-filled fiber was slightly multimode (the used fiber structure is optimized for good transmission properties when empty), an emission on a single quasi Gaussian mode was possible [14]. The real mode shape revealed the hexagonal symmetry of the cladding structure. We also showed that the temporal shape of the pulses can be perfectly explained by a quasi-steady-state regime modeling of the Raman mechanisms, i.e., instantaneous response of the Raman effect at the pulse duration time scale [15,16]. We experimentally measured a long-term stability only limited by the pump beam stability [15]. All these characteristics have been observed for different liquids at different Stokes wavelengths [16]. After these proofs of principle we propose to build in the present work an efficient Raman converter emitting in the yellow range at the target wavelength of 583 nm. Indeed this wavelength is interesting for biological applications since it matches an absorption line of several fluorophores, such as Bodipy 581/591 or X-Rhodamine for example [1,2]. We describe first the design of this new converter. The choice of the active Raman liquid, the mixture of liquids to be used to adjust the refractive index, and the band position is discussed. Then we present the experimental setup and the results. The internal conversion efficiency from the pump at 532 nm to the target wavelength at 583 nm is high (67% in photon numbers) despite working on the second Stokes order of the Raman cascade. The new wavelength is emitted in a quasi-Gaussian spatial beam with a high spectral brightness.

2. DESIGN OF THE RAMAN CONVERTER EMITTING AT 583 nm

The Raman converter is based on the Amplified Spontaneous Emission principle, photons emitted through spontaneous Raman scattering being further amplified by stimulated Raman scattering. It is thus very simply implemented, requiring just a pump operating in a single pass scheme in the nonlinear medium. Liquids, just as any material, present complex Raman spectra with many lines among which the one with the highest Raman gain coefficient g_{R1} is called the main Raman line. Other lines with lower Raman gain coefficients g_{Ri} are called secondary Raman lines. For a given line, the Raman threshold can be defined when the parameter $\gamma = g_R \frac{P_p \times L}{A_{\text{eff}}}$ is approximately equal to 25 [17]. g_R is the Raman gain coefficient, P_p is the internal peak pump power, A_{eff} is the effective area, and L is the interaction length. When increasing P_p and assuming no losses, before its saturation the Stokes power varies as $\exp(\gamma)$. So, around threshold, if $\frac{g_{Ri}}{g_{R1}} \lesssim 0.7$, the Stokes power of the main line will be more than 1800 times higher than the Stokes power of the secondary Raman line. So we propose this value of 0.7 as a good criterion to say that, as we are working in the steady-state regime, Stimulated Raman Scattering (SRS) occurs on the main Raman line only, secondary lines emission being neglected. Above threshold the pump begins to be depleted by energy transfer toward the main line, and no more power is available to amplify the secondary lines, increasing again the effect. When $\frac{g_{Ri}}{g_{R1}}$ becomes close to unity, it is difficult to identify the main Raman line from a secondary line.

In this case competition occurs between the two lines, and a solution to favor one line is to put extra-losses on the other one. Indeed the amplification gain of the unwanted line varies as $\exp(\gamma - \alpha L)$, where α represents the linear losses and hence vanishes when $\gamma < \alpha L$.

In this work we want to shift the pump wavelength at 532 nm to the target wavelength of 583 nm by using SRS in a liquid. Such a wavelength shift corresponds to a Raman shift around 1640 cm^{-1} which is not directly achievable with the common and non-harmful Raman liquids we want to use [18,19]. It also corresponds to the second Stokes order of a line with a Raman shift around 820 cm^{-1} . This shift matches with a Raman line of alcohols. To choose the most convenient alcohol, we have to calculate the Raman gain coefficients. For that, we have used the formula demonstrated in Ref. [20] and considered the depolarization ratio ρ_S , which adds a correction factor of $\frac{1}{1+\rho_S}$ to it [21]. This formula becomes:

$$g_R = \frac{1}{1 + \rho_S} \frac{8\pi}{\Delta\nu_{\text{FWHH}}} \frac{Nc^2}{\omega_S^3 \hbar n_S^2} \left(\frac{\partial\sigma}{\partial\Omega} \right). \quad (1)$$

For the liquids and lines we use in this work, ρ_S is much smaller than one and brings only a minor correction, but has to be considered in some other liquids or lines. $\Delta\nu_{\text{FWHH}}$ is the full width at half height of the spontaneous Raman line, N is the molecular density, c is the velocity of light, ω_S and n_S are the Stokes frequency and refractive index. $\frac{\partial\sigma}{\partial\Omega}$ is the total differential scattering cross-section [22]. In Ref. [23] this cross-section is given for a pump wavelength of 488 nm. As this parameter is wavelength dependent, we have to calculate it for the wavelengths we are interested in according to the following formula [24]:

$$\frac{\partial\sigma}{\partial\Omega} = \frac{A\omega_p^4}{(\omega_i^2 - \omega_p^2)^2}. \quad (2)$$

A is a constant of proportionality, ω_p is the pump frequency, ω_s is the Stokes frequency, and ω_i is a UV material resonance frequency. In the liquids that we study, $\omega_p \ll \omega_i$, so we can consider that $\frac{\partial\sigma}{\partial\Omega}$ is proportional to the fourth power of ω_s .

In alcohols there are usually two strong Raman bands, one around $2800\text{--}3000 \text{ cm}^{-1}$ (denoted as band I in the following) and one around $800\text{--}1040 \text{ cm}^{-1}$ (denoted as band II). Each band contains several Raman lines. In Tables 1 and 2, we have computed the Raman gain coefficients g_R in several alcohols for the strongest Raman line in band I (denoted $g_{R,I}$) and for the strongest Raman line in band II (denoted $g_{R,II}$) from the figures published in Refs. [23,25] at the pump wavelength λ_p of 532 nm. We calculated $g_{R,II}$ for the first Stokes order emitting at λ_{1s} ($g_{R,II}$ at λ_p), for the second Stokes order emitting at λ_{2s}

Table 1. Estimated Raman Gains (in $\times 10^{12} \text{ W}^{-1} \text{ m}$) of Different Alcohols for the Strongest Raman Line in Band I^a

Liquid	Raman Shift (cm^{-1})	λ_{1s} (nm)	$g_{R,I}$ at λ_p
Methanol	2837	626	2.16
Ethanol	2928	630	2.92
Propan-2-ol	2882	628	2.43

^aThe pump wavelength is $\lambda_p = 532 \text{ nm}$. λ_{1s} is the wavelength of the first Stokes order.

Table 2. Estimated Raman Gains (in $\times 10^{12} \text{ W}^{-1} \text{ m}$) of Different Alcohols for the Strongest Raman Line in Band II^a

Liquid	Raman Shift (cm ⁻¹)	λ_{1s} (nm)	λ_{2s} (nm)	$g_{R,II}$ at λ_p	$g_{R,II}$ at λ_{1s}	$g_{R,II}$ at λ_{1s}
Methanol	1037	563	598	0.57	0.54	0.25
Ethanol	881	558	587	1.04	0.99	0.34
Propan-2-ol	819	556	583	2.50	2.37	0.97

^aThe pump wavelength is $\lambda_p = 532 \text{ nm}$. λ_{1s} (λ_{2s}) is the wavelength of the first (second) Stokes order.

($g_{R,II}$ at λ_{1s} , λ_{1s} being the pumping wavelength), and finally for the ratio $\frac{g_{R,II} \text{ at } \lambda_{1s}}{g_{R,I} \text{ at } \lambda_p}$.

In methanol and ethanol, the ratio $\frac{g_{R,II} \text{ at } \lambda_{1s}}{g_{R,I} \text{ at } \lambda_p}$, is largely below 0.7, so we expect that SRS will occur on the Raman line of band I only. Propanol has two isomers, propan-1-ol and propan-2-ol. In the literature we did not find values of Raman cross sections in propan-1-ol, so we are not able to calculate the Raman gain. However, in Refs. [26,27] the authors both evaluated that the intensity of the Raman line at 2876 cm^{-1} is higher than the intensity of the Raman line at 860 cm^{-1} . This assumption is also stressed by a visual comparison of the Raman spectrum of propan-1-ol with the Raman spectrum of ethanol, showing the same global trends [19]. This makes us believe that the strongest line in band I is the main Raman line in propan-1-ol, similarly for methanol and ethanol, and will be strongly favored at the expense of band II.

For propan-2-ol, more data are available in the literature and they enable us to calculate the Raman gains [23,25]. As can be seen in Table 1 the Raman line of propan-2-ol at 2882 cm^{-1} has a gain of $2.43 \times 10^{-12} \text{ W}^{-1} \text{ m}$. As can be seen in Table 2 the Raman line at 819 cm^{-1} has a gain of $2.50 \times 10^{-12} \text{ W}^{-1} \text{ m}$ for the first Stokes order and a gain of $2.37 \times 10^{-12} \text{ W}^{-1} \text{ m}$ for the second Stokes order we want to generate.

Contrary to the other alcohols studied, in propan-2-ol, $\frac{g_{R,II} \text{ at } \lambda_{1s}}{g_{R,I} \text{ at } \lambda_p}$ is very close to unity. So in comparison with ethanol, methanol, and propan-1-ol this liquid is the most favorable for SRS emission on the 819 cm^{-1} line. As $g_{R,II}$ in propan-2-ol is almost the same as $g_{R,I}$ in ethanol for which we already demonstrated SRS in ethanol in a Raman converter on the 2928 cm^{-1} line [14,15], we are confident that it will be high enough to generate SRS in this new converter. So we decided to use propan-2-ol to generate SRS on the second Stokes order of the line at 819 cm^{-1} . Our objective is then twofold: 1) to stop the Raman cascade at the second Stokes order of the line at 819 cm^{-1} in order to optimize the pump transfer energy on the target wavelength, and 2) to prevent SRS on the line at 2882 cm^{-1} by adding extra-losses on it.

We have used a 1 m long HC-PCF with a transmission band centered around $1 \mu\text{m}$ (ref. NKT Photonics, HC 1060-02). In order to shift the transmission band around 580 nm, the fiber has to be filled with a liquid having a refractive index around 1.39 [13,16]. As the refractive index of propan-2-ol is 1.37, one needs to mix it with a high index liquid. We have chosen to use DMSO (Dimethyl Sulfoxide) as the diluent, as it mixes well

with alcohols and its refractive index is 1.48, allowing us to keep a high proportion of the alcohol in the mixture. The proportions of the liquids were 11% of DMSO and 89% of propan-2-ol in volume. This weak dilution ensures that the Raman gain of DMSO in the mixture remains much smaller than the Raman gain of propan-2-ol in the mixture, so that the converter will not emit on a Raman line of DMSO. The refractive index of the mixture is firstly measured with an Abbe refractometer at 589 nm. Then a small piece of fiber (5 cm) is filled with the mixture to measure the transmission band by injecting the light of a supercontinuum laser in it. At the output of this small piece of fiber, we collect and filter the light that comes from the core before sending it to the optical spectrum analyzer (OSA). Some adjustments of the liquid index are sometimes necessary, and once the transmission band is satisfactory we fill the fiber of the converter with the liquid thanks to a homemade microfluidic system. Both ends are hermetically closed with micro-tanks [28]. The whole device “liquid HC-PCF + tanks” is called the “Raman converter” (see insert of Fig. 2). The transmission bandwidth of the converter may be slightly narrower than the one of the small piece of fiber because of the filtering of the modes along the length of propagation (typically 1 m). Another fine adjustment of the liquid index may be necessary. In Fig. 1, we show three transmission bands of the same fiber, being filled with a liquid mixture having successively a refractive index of 1.384, 1.388, and 1.394. Between two fillings our microfluidic system enables us to rinse the fiber to ensure the mixture of liquids is the expected one. The transmission bands were registered by optimizing the level of the output signal of the converter at 532 nm. We can estimate from Fig. 1 that the right band edge of the transmission band shifts with a rate of roughly 5 nm for a change in the refractive index of 10^{-3} in the range of indices we use. This estimation is helpful to optimize the position of the transmission band with the refractive index of the liquid mixture. The transmission band is optimized to contain the pump line at 532 nm, the first Stokes order line at 556 nm, and the second Stokes order line at 583 nm. The third Stokes order at 612 nm and the first Stokes order at 628 nm of the line at 2882 cm^{-1} have to be out of the transmission band, so that these lines will not be generated efficiently. From Fig. 1, we can see that

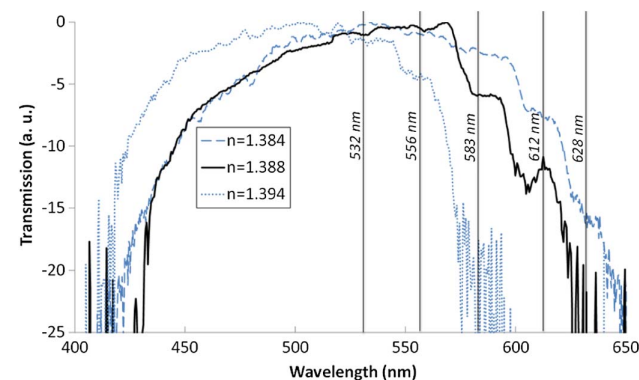


Fig. 1. Optimization of the transmission band of a 1 m long HC-PCF 1060-02 filled with a mixture of propan-2-ol and DMSO. The refractive index of the liquid mixture is, respectively, 1.384 (dashed line), 1.388 (full line), and 1.394 (dotted line).

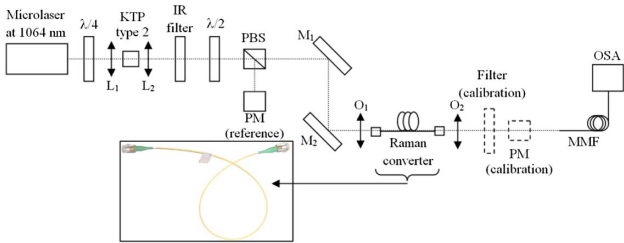


Fig. 2. Experimental setup. The $\lambda/4$ plate enables us to optimize the conversion efficiency of the IR beam to 532 nm in the type 2 KTP crystal. L1, focalizing lens; L2, collimating lens. The $\lambda/2$ plate associated with the polarizing beam splitter (PBS) enables us to vary the incident pump power. The rejected beam is sent to a powermeter (PM reference) to serve as a pump power reference. M1, M2, mirrors; O1, O2, microscope objectives; MMF, multimode fiber; OSA, optical spectrum analyzer. In the dashed line, a removable colored filter and powermeter (PM calibration) were used for the power calibration. Insert: photo of the Raman converter.

converter with $n = 1.394$ is not optimized since the line at 583 nm suffers from too many losses. We have tested the two other converters ($n = 1.384$ and $n = 1.388$) and will present the best results obtained with the converter having $n = 1.388$.

3. EXPERIMENTAL SET-UP

The experimental set-up is depicted in Fig. 2. We have used a frequency-doubled microlaser emitting at 532 nm as the pump source, with a pulse duration of 560 ps (FWHM). The frequency rate repetition is 5.6 kHz, and the maximum mean pump power incident on the converter is 5.75 mW (corresponding to a peak power of 1.8 kW and an energy per pulse of 1 μ J). The pump beam is focused inside the Raman converter through a microscope objective ($\times 6.3$, NA 0.2). At the output of the Raman converter, we collect the light through a second microscope objective ($\times 6.3$, NA 0.2). The light is sent in an OSA through a multimode fiber. We measured the power of the different lines emitted by the Raman converter by sending the output beam through a multimode fiber in an OSA used with a low resolution of 10 nm, much larger than the Raman linewidths. The power calibration of the system “multimode fiber + OSA” is firstly made by measuring the power in mW of the different wavelengths taken separately thanks to colored filters, put just before the multimode fiber. Knowing the transmission of the colored filters, we can deduce the power in mW of the different wavelengths at the output of the converter. Then for each wavelength a mean power in the arbitrary unit is calculated from the OSA and can be converted into the power in mW at the output of the converter. Within this method we can have simultaneous measurements of the powers of each wavelength delivered by the Raman converter.

4. RESULTS

In Fig. 3 we show an example of the transmitted powers of the different lines delivered by the converter versus the incident pump power P_{in} at 532 nm. The injection of the pump beam in the converter was first optimized for low pump powers,

before the threshold of the first Stokes order at 556 nm. The pump injection efficiency is then estimated to be 30%. Then we increased P_{in} until the appearance of the first Stokes order at 556 nm for $P_{\text{in}} = 1.5$ mW. Slightly moving the injection microscope enables us to optimize the output powers but sometimes led to irreversible damage of the converter (probably due to the burning of impurities or dusts at the input of the converter), so we chose not to optimize the output power at 556 nm as it was not the target wavelength. This explains why the power at 556 nm does not grow higher. By continuing to increase P_{in} we observed the appearance of the second Stokes order at 583 nm for $P_{\text{in}} = 3$ mW. The first Stokes order saturated, and the second Stokes order then grew without any saturation. Just before the maximum incident pump power we carefully optimized the output power at 583 nm and obtained a power of 1.06 mW for the maximum pump power of 5.75 mW. It corresponds to a maximum peak power of 338 W at 583 nm and an energy of 0.19 μ J per pulse. The internal conversion efficiency from the internal pump power to the second Stokes order at 583 nm is 61% (or 67% in photon numbers). For high pump powers, we observed that the pump and the first Stokes order at 556 nm are not completely depleted which has been previously explained by the Gaussian temporal shape of the pump pulse [15,16]. At maximum pump power we observed the onset of the third Stokes order at 612 nm in a core mode and the onset of the first Stokes order of the line in band I at 628 nm in a cladding mode, but the powers were very weak (about a few μ W). This illustrates the difficulty of improving the adjustment of the transmission band but also shows the efficiency of the SRS in the converter.

The highest achievable resolution of the OSA we used in the present experiment was 50 pm which is in the range of the Raman spectral linewidths of liquids. So even if it was not possible to precisely measure the linewidths of the emitted lines we had an upper limit of these values. Insert in Fig. 3 shows an example of the spectrum of the line at 583 nm obtained at the highest resolution of the OSA. To get a more precise value we used the fact that the spectral width of the Stokes output $\Delta\omega_{1/2}$ (FWHH) narrows with the gain according to the following formula [29]:

$$\Delta\omega_{1/2} \cong \left(\frac{\ln 2}{2\gamma \times L} \right)^{1/2} \Gamma. \quad (3)$$

L is the length of the converter, and Γ is the spontaneous spectral linewidth (FWHH). We took $L = 1$ m and $\Gamma = 6.6 \text{ cm}^{-1}$ [25]. To calculate γ we took $P_p = 59 \text{ W}$ (see Fig. 3). We approximate the Raman gain of propan-2-ol in the mixture by simply multiplying its value obtained in Table 2 for its pure form by its proportion in the mixture, i.e., 89%. We obtained $g_R = 2.11 \times 10^{-12} \text{ W}^{-1} \text{ m}$. For A_{eff} we took the value measured in a previous work in a Raman converter built with the same HC-PCF and filled with ethanol [14], i.e., $12 \times 10^{-12} \text{ m}^2$. Then, we found that $\Delta\omega_{1/2} = 1.2 \text{ cm}^{-1}$ (corresponding to 47 pm). The estimated spectral power density at 583 nm is 22 mW/nm, which is well above the one obtained in this spectral range by sub-ns supercontinuum sources, typically 700 μ W/nm in the MHz range (among

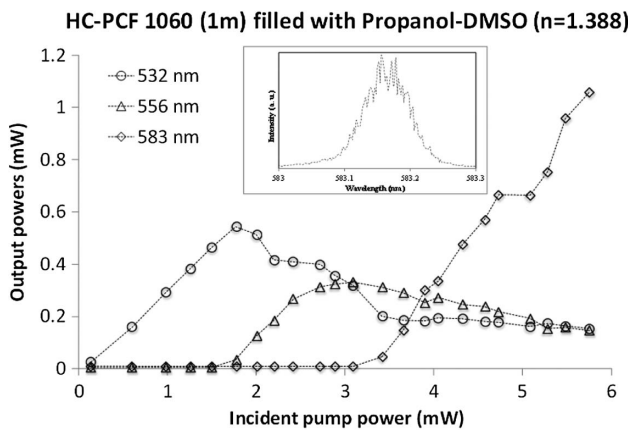


Fig. 3. Mean output powers of the different lines emitted by the Raman converter at 583 nm versus the mean incident pump power. Insert: example of spectrum of the line at 583 nm at the highest resolution of the OSA.

the references of [4–6] a spectral power density of 4 mW/nm has been obtained but in the ps regime).

The output beam of the converter was sent on a diffraction grating after which we observe the spatial patterns of the modes projected on a screen [Fig. 4(a)]. On this saturated image we can see the typical shape of the modes of HC-PCF fibers with an hexagonal symmetry due to the structure of the cladding. The periodic structure of the holes in the cladding is also responsible for the presence of petal lobes around the core. These petal lobes can be seen as part of the fundamental mode and carry only a very small percentage of the energy. On the far-field patterns of Figs. 4(b) and 4(c) we can see that the Stokes lines at 556 and 583 nm are emitted in quasi-Gaussian modes.

From simulations of the Raman cascade [15] and from previous experimental studies [30] we can estimate that the temporal pulse duration at 583 nm is shorter than the pump pulse duration (i.e., 560 ps FWHM). An order of magnitude of this pulse duration at maximum pump power is expected to be around 100–200 ps FWHM by the numerical simulations.

In this work we have shown that the exploitation of the various Raman lines of common liquids and the adjustment of

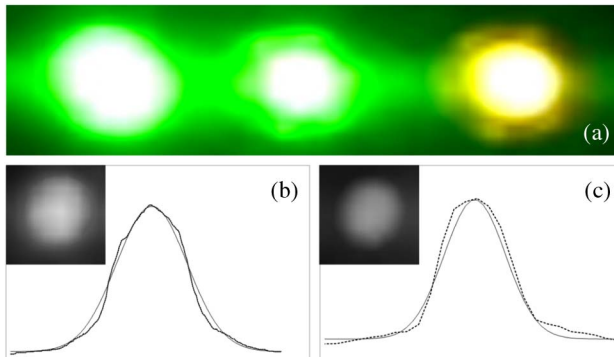


Fig. 4. (a) Spatial modes at 532 nm, 556 nm, and 583 nm (from left to right) at the output of the Raman converter around maximum incident pump power. (b) Example of far field pattern of the line at 556 nm. (c) Example of a far field pattern of the line at 583 nm (dotted line: experimental data, full line: Gaussian fit).

the refractive index of the liquid mixtures to finely control the position of the transmission bands broaden the possibilities of our Raman converters. A simple microlaser at 532 nm associated with different Raman converters will enable us to access “on demand” discrete wavelengths with high conversion efficiencies in beams with high spectral brightness and good spatial quality, opening new opportunities in, for example, biological applications.

5. CONCLUSION

We have designed, built, and characterized a Raman converter emitting at 583 nm on the second Stokes order of a line of propan-2-ol pumped by a microlaser at 532 nm in the sub-nanosecond regime. The internal conversion efficiency is 67% in photon numbers and the output power is 1.06 mW, corresponding to a maximum peak power of 338 W. The beam delivered by the converter presents a Gaussian spatial structure and a spectral brightness more than five times higher than supercontinuum sources in this spectral range. The principle of this Raman converter can be adapted to other Raman liquids to deliver other wavelengths in the visible range. These Raman converters have applications in areas such as fluorophore excitation where pulsed low energies at specific discrete wavelengths are needed. Moreover the liquid mixtures method offers a new degree of freedom for the study of other nonlinear effects. For example, it may enable us to adjust the position of the zero-dispersion wavelength to realize a phase-matching condition in a four-wave mixing process for the generation of correlated photon pairs [31].

Funding. Fondation Coopération Scientifique Paris Saclay.

Acknowledgment. The authors thank the “Fondation Coopération Scientifique Campus Paris-Saclay” for supporting the work of Minh Châu Phan Huy.

REFERENCES

1. <http://www.thermofisher.com/fr/fr/home/life-science/cell-analysis/labeling-chemistry/fluorescence-spectraviewer.html>.
2. <https://www.biotech.iastate.edu/facilities/flow/Fluorochromes.pdf>.
3. J. Spinhirn, “Micro pulse lidars,” IEEE Trans. Geosci. Remote Sens. **31**, 48–55 (1993).
4. <https://www.leukos-systems.com/our-products/supercontinuum-lasers/scientific/new-wave>.
5. <https://www.nktphotonics.com/lasers-fibers/product/superk-extreme-supercontinuum-lasers/>.
6. <http://www.yslphotonics.com/Home/Index/Product/index/id/24.html>.
7. http://www.elforlight.com/_products/opo_03.htm.
8. T. Omatsu, A. Lee, H. M. Pask, and J. Piper, “Passively Q-switched yellow laser formed by a self-Raman composite Nd:YVO₄/YVO₄ crystal,” Appl. Phys. B **97**, 799–804 (2009).
9. G. Fanjoux, A. Sudirman, J. C. Beugnot, L. Furfaro, W. Margulis, and T. Sylvestre, “Stimulated Raman-Kerr scattering in an integrated nonlinear optofluidic fiber arrangement,” Opt. Lett. **39**, 5407–5410 (2014).
10. S. Yiou, P. Delaye, A. Rouvie, J. Chinaud, R. Frey, G. Roosen, P. Viale, S. Février, P. Roy, J.-L. Auguste, and J.-M. Blondy, “Stimulated Raman scattering in an ethanol core microstructured optical fiber,” Opt. Express **13**, 4786–4791 (2005).
11. R. F. Cregan, B. J. Mangan, J. C. Knight, T. A. Birks, P. St. J. Russell, P. J. Roberts, and D. C. Allan, “Single-mode photonic band gap guidance of light in air,” Science **285**, 1537–1539 (1999).

12. Y. Y. Wang, F. County, P. S. Light, B. J. Mangan, and F. Benabid, "Compact and portable multiline UV and visible Raman lasers in hydrogen-filled HC-PCF," *Opt. Lett.* **35**, 1127–1129 (2010).
13. G. Antonopoulos, F. Benabid, and T. A. Birks, "Experimental demonstration of the frequency shift of bandgaps in photonic crystal fibers due to refractive index scaling," *Opt. Express* **14**, 3000–3006 (2006).
14. S. Lebrun, P. Delaye, R. Frey, and G. Roosen, "High-efficiency single-mode Raman generation in a liquid-filled photonic bandgap fiber," *Opt. Lett.* **32**, 337–339 (2007).
15. S. Lebrun, C. Buy, P. Delaye, R. Frey, G. Pauliat, and G. Roosen, "Optical characterizations of a Raman generator based on a hollow core photonic crystal fibre filled with a liquid," *J. Nonlinear Opt. Phys. Mater.* **19**, 101–109 (2010).
16. S. Lebrun, M. C. Phan Huy, P. Delaye, and G. Pauliat, "Efficient stimulated Raman scattering in hybrid liquid-silica fibers for wavelength conversion," *Proc. SPIE* **10021**, 1002104 (2016).
17. M. C. Phan Huy, P. Delaye, G. Pauliat, N. Dubreuil, F. Gérôme, B. Debord, F. Benabid, and S. Lebrun, "Lowering backward Raman and Brillouin scattering in waveguide Raman wavelength converters," *J. Eur. Opt. Soc.* **13**, 31 (2017).
18. M. D. Martin and E. L. Thomas, "Infrared difference frequency generation," *IEEE J. Quantum Electron.* **2**, 196–201 (1966).
19. Spectral Database for Organic Compounds (SDBS), http://sdbs.db.aist.go.jp/sdbs/cgi-bin/direct_frame_top.cgi.
20. M. Maier, W. Kaiser, and J. A. Giordmaine, "Backward stimulated Raman scattering," *Phys. Rev.* **177**, 580–599 (1969).
21. S. Porto, "Angular dependence and depolarization ratio of the Raman effect," *J. Opt. Soc. Am.* **56**, 1585–1589 (1966).
22. L. Shan, G. Pauliat, G. Vienne, L. Tong, and S. Lebrun, "Design of nanofibres for efficient stimulated Raman scattering in the evanescent field," *J. Eur. Opt. Soc.* **8**, 13030 (2013).
23. J. E. Griffiths, "Raman scattering cross sections in strongly interacting liquid systems: CH₃OH, C₂H₅OH, i-C₃H₇OH, (CH₃)₂CO, H₂O, and D₂O," *J. Chem. Phys.* **60**, 2556–2557 (1974).
24. W. K. Bischel and G. Black, "Wavelength dependence of Raman scattering cross sections from 200–600 nm," in *Excimer Lasers*, C. K. Rhodes, H. Egger, and H. Pummer, eds. (American Institute of Physics, 1983), pp. 181–187.
25. M. J. Colles and J. E. Griffiths, "Relative and absolute Raman scattering cross sections in liquids," *J. Chem. Phys.* **56**, 3384–3391 (1972).
26. K. Krishnan, "The Raman spectra of organic compounds, Part I Methyl, Ethyl, n-Propyl and n-Butyl Alcohols," *Proc. Indian Acad. Sci. A* **53**, 151–167 (1961).
27. R. W. Wood and G. Collins, "Raman spectra of a series of normal alcohols and other compounds," *Phys. Rev.* **42**, 386–392 (1932).
28. S. Lebrun, M. C. Phan Huy, P. Delaye, and G. Pauliat, "Optical device having a liquid-core optical fibre and method for producing such a device," European patent FR2996011 (A1) (21 September 2012).
29. C.-S. Wang, "Theory of stimulated Raman scattering," *Phys. Rev.* **182**, 482–494 (1969).
30. L. Shan, G. Pauliat, G. Vienne, L. Tong, and S. Lebrun, "Stimulated Raman scattering in the evanescent field of liquid immersed tapered nanofibers," *Appl. Phys. Lett.* **102**, 201110 (2013).
31. M. Barbier, I. Zaquine, and P. Delaye, "Spontaneous four-wave mixing in liquid-core fibers: towards fibered Raman-free correlated photon sources," *New J. Phys.* **17**, 053031 (2015).